SPWLA 66th Annual Logging Symposium, May 17-21, 2025
DOI: 10.30632/SPWLA-2025-0004

A NOVEL HIERARCHIAL CORRECTION OF ARRAY INDUCTION LOGGING DATA FOR HORIZONTAL WELLS IN TIGHT SANDSTONE RESERVOIRS

Ping Qiao[1,2], Lei Wang[1,2*], Yingming Liu[3], Xiaokai Xu[4], Xiyong Yuan[4], Fuhua Cao[1,2]

1. National Key Laboratory of Deep Oil and Gas, China University of Petroleum (East China), Qingdao 266580;
2. School of Geosciences, China University of Petroleum (East China), Qingdao 266580;
3. Research Institute of Petroleum Exploration & Development, PetroChina, Beijing 100083;
4. Geological and Measurement Control Technology Research Institute, Sinopec Matrix Corporation, Qingdao 266001.

ABSTRACT

Array induction logging (AIL) is widely used for post-drilling measurements in horizontal (HZ) wells due to its multiple radial detection depths, high vertical resolution, and cost-effectiveness. However, the core algorithm of AIL, known as "software focusing" SF, is optimized for vertical wells, resulting in a weak focusing effect in HZ wells. This can lead to unexpected responses separation and resistivity horns with apparent values significantly exceeding the true resistivity. In tight sandstone reservoirs, the effects of dipping angle, mud invasion, and resistivity anisotropy are coupled, leading to extremely complicated tool responses. Unfortunately, existing resistivity correction methods are limited to deviated wells with relative dipping below 80 degrees. Therefore, the development of accurate and efficient processing of AIL data for HZ wells in tight sandstone reservoirs is imperative.

The main challenge in processing AIL data for HZ wells lies in simulating the tool responses within a three-dimensional (3D) environment. The slow modeling speed, numerous inversion parameters, and limited measured curves make implementing a 3D inversion impractical for AIL data. To tackle this challenge, a novel hierarchical correction method for AIL data in HZ wells within tight sandstone reservoirs has been introduced in this paper. The essence of this new approach is to separate the influences of anisotropy and invasion in HZ wells, simplifying the complex 3D model into a combination of horizontal layered (1D) and cylindrical layered (1D) models.

First, this paper established a coefficient library of true thickness correction based on a horizontal layered model to eliminate the effect of thickness, and the horizontal layered model is then simplified into a homogenous (0D) model. On this basis, a direct focusing algorithm for radial focused responses is introduced for the 0D model, improving the forward modeling speed. Furthermore, the responses after true thickness correction are input into the cylindrical layered model to correct the invasion effect. In addition, the anisotropy coefficient is determined by the measured responses of HZ well and the vertical section of the HZ well. Finally, the result of the invasion correction was input into the 0D model to complete the anisotropy correction. The new method significantly reduces the complexity of the inversion model and allows fast and accurate processing of AIL data for HZ wells in tight sandstone reservoirs.

Validation with measured data demonstrates that the new method achieves a processing speed of four points per second, with accuracy errors controlled within 3%, meeting the needs of real-time inversion. Meanwhile, the new method can accurately characterize the invasion and extract the electrical parameters of tight sandstone reservoirs, which lays a solid foundation for fluid identification and reservoir evaluation.

INTRODUCTION

Tight sandstone reservoirs in China hold substantial reserves and represent a critical strategic alternative to conventional hydrocarbon resources. These reservoirs exhibit electrical anisotropy due to depositional heterogeneity and oriented fracture networks (Anderson et al., 1995; Bang et al., 2001; Hagiwara, 2011). During drilling operations, mud-filtrate invasion (Alpak et al., 2003; Zhou et al., 2016) and thin-bedding effects (Mallan and Torres-Verdín, 2007; Liu et al., 2020) significantly distort resistivity measurements, while coupled environmental factors complicate data interpretation (Rabinovich et al., 2006; Wang, 2009).

These challenges necessitate advanced methodologies for accurate electrical parameter extraction in tight sandstone evaluation.

The global oil industry increasingly employs horizontal (HZ) wells for unconventional reservoir development. Chinese operators predominantly utilize post-drilling resistivity inversion for reservoir characterization (Gao et al., 2007; Qiu et al., 2022), with array induction logging (AIL) being the primary measurement technology due to its multiple investigation depths and vertical resolution (Barber and Rosthal, 1991; Beard et al., 1996; Beste et al., 2000). However, the vertical-well-optimized software focusing (SF) algorithm demonstrates limited efficacy in HZ wells (Gorbatenko et al., 2016; Li et al., 2019), resulting in resolution inconsistencies, resistivity deviations, and characteristic horn effects (Zhou et al., 1994; Bai et al., 2018). Furthermore, complex interactions between wellbore deviation, formation anisotropy, and invasion profiles (Tarouilly et al., 2003; Løseth and Ursin, 2007) substantially compromise interpretation accuracy.

Current AIL correction methodologies for HZ wells face two principal limitations: 1) dip-adaptive filtering techniques (He et al., 2012; Hou and Bittar, 2010) sacrifice accuracy for real-time processing capability, and 2) 1D inversion-based approaches (Hong et al., 2021; Wang et al., 2023) lack applicability beyond simple horizontal formations. Both methods exhibit degraded performance beyond 80° deviation angles (Wang et al., 2022; Zhou et al., 2016), highlighting critical gaps in HZ well interpretation.

The technical challenges stem from three fundamental constraints: computationally intensive 3D modeling (Løseth and Ursin, 2007; Hong et al., 2021), high-dimensional parameter spaces (Rabinovich et al., 2006; Wang, 2009), and limited measurement sensitivity. This study proposes a hierarchical correction framework that decouples anisotropy and invasion effects through model dimensionality reduction. The methodology sequentially combines: 1) True-thickness correction via horizontal-layer modeling, 2) Radial-focused response computation using accelerated 0D forward modeling, 3) Invasion profile reconstruction through cylindrical-layer inversion, and 4) Anisotropy correction calibrated with vertical-section data.

Field applications demonstrate the method's capability to process 4 data points per second with <3% relative error, achieving real-time inversion requirements. The technique accurately resolves invasion profiles and extracts formation electrical parameters, providing reliable inputs for fluid identification and reservoir assessment. This advancement establishes a practical workflow for tight sandstone evaluation in complex HZ well environments.

METHOD AND THEORY

The array induction logging tool (taking HDIL as an example) is composed of 7 sub-arrays. The main transmitter generates an alternating electromagnetic field with 8 frequencies in the formation. Then, 7 receivers with different spacings are used to measure the induced electromotive force caused by the currents in the formation, thereby obtaining a total of 56 conductivity signals. After skin effect correction, borehole correction, and SF processing, focused responses with 3 fixed vertical resolutions (1, 2, and 4 ft) and 6 different radial detection depths (10, 20, 30, 60, 90, and 120 inches) can be obtained. Each sub-array of the HDIL tool adopts a basic three-coil system. The structure of the tool and its data preprocessing flow are shown in **Fig. 1**.

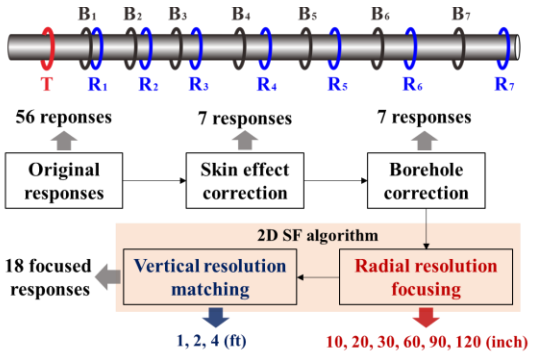

Fig. 1—Structure of the HDIL tool and its data preprocessing flow.

The SF algorithm consists of two components, radial resolution focusing and vertical resolution matching. The principle of the SF algorithm is that the formation is assumed to be rotationally symmetric, in which case the conductivity can be viewed as a function of the radial and vertical depth. Digital signal processing and inversion algorithms are employed to process the original responses of sub-arrays. According to the geometric parameters of different coils, spacings, and the electromagnetic characteristics of the formation, the response functions corresponding to each receiver with different detection depths and vertical resolutions are calculated. Through weighted summing these response functions, the weights of responses for different positions are adjusted, the responses of the target region are enhanced, sidelobe and interference signals are

suppressed, and the response focusing is achieved. The response focusing can be described mathematically as,

$$\sigma_p(\rho_k, z) = \sum_{j=1}^{J} \sum_{z'=z_{\min}}^{z_{\max}} w_j^k(z', \sigma)\sigma_a^j(z - z'), \quad (1)$$

where $\sigma_p(\rho_k, z)$ is the conductivity at the radial position ρ_k and the vertical position z after focusing, and the k is the number of detection depths focused, $k = 1, \ldots, 6$. $\sigma_a^j(z)$ is the response of j-th subarray at z, $j = 1, 2, \ldots, 7$. $w_j^k(z', \sigma)$ is the filter of the j-th subarray when the detection depth is ρ_k, and $z = z_{\min} \sim z_{\max}$ is the vertical distance of the focusing.

RESPONSE CHARACTERISTICS IN HZ WELLS

The establishment of an efficient processing method for AIL data in tight sandstone reservoirs of HZ wells hinges on accurately grasping the response characteristics of AIL in such complex environments. To achieve this goal, it is essential to thoroughly analyze the sensitivity of AIL responses to various parameters, thereby clarifying the specific impacts of each factor on the responses. Based on this, this section will conduct a detailed analysis of the sensitivity of AIL responses to anisotropy, invasion, and layer thickness respectively. The aim is to comprehensively and deeply reveal the response laws of AIL in the tight sandstone reservoirs of horizontal wells, providing a solid foundation for the construction of subsequent efficient processing. Since the SF algorithm of HDIL tool has not been disclosed, this paper realizes the responses focusing by using commercial software Express.

Sensitivity of AIL Responses to Anisotropy

Anisotropy causes the AIL responses to deviate from the true resistivity. Therefore, clarification of the characteristic laws of AIL focused responses in HZ wells within anisotropic formations is an essential prerequisite for accurate processing of such data. To this end, this section considers the influence of the dipping angle and anisotropy, adopts a homogeneous model and analyses the sensitivity of the AIL responses. **Fig.2** shows the focused responses with different dipping angles α and anisotropy coefficients λ in a homogeneous model with horizontal resistivity R_h of 30 Ω·m, where $\lambda = \sqrt{R_v / R_h}$ and R_v is the vertical resistivity.

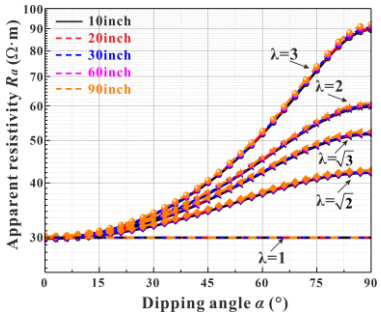

Fig. 2—Focused responses under anisotropic formations with different λ.

As can be seen from the **Fig. 2**, with the increase of α, the contribution of vertical resistivity R_v to apparent resistivity R_a is increasing, resulting in the measured responses rising, and the degree of rising is proportional to the λ. Additionally, the responses of a single dipping angle cannot accurately characterize the anisotropy, and the information of multiple angles is needed to determine the anisotropy coefficient. Another point to note is that anisotropy rarely separates the depth responses.

In order to further verify the accuracy of the above conclusions, we first established an isotropic three-layer model of HZ wells. The dipping angle of the model is 89°, the resistivities of the surrounding rock on both sides and middle layer are 20 Ω·m and 40 Ω·m, and the thickness H of middle layer is 5m. **Fig. 3 (a)** shows the focused responses of the model. On this basis, the isotropic model is modified into anisotropic model with an anisotropic coefficient of $\sqrt{2}$. The response of the modified anisotropic model is shown in **Fig. 3 (b)**.

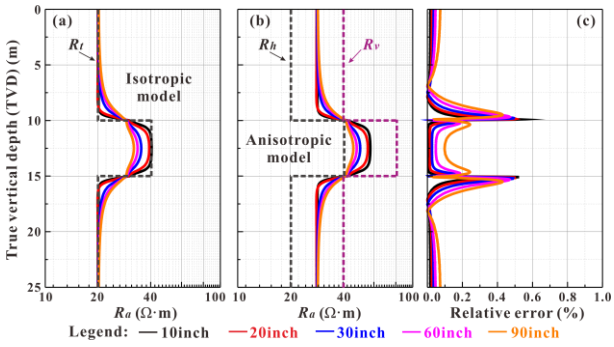

Fig. 3—Comparison of responses in an isotropic model with responses in an anisotropic model when α= 89°: (a) Responses in an isotropic model; (b) Responses in an anisotropic model; (c) Relative error between the responses of Fig. (b) divided by the anisotropy coefficient and responses of Fig. (a).

By comparing **Fig. 3 (a)** and **Fig. 3 (b)**, it can be found that the response shape of the two is the same, but the overall value has changed. The response of the anisotropic model as a whole is divided by the anisotropy coefficient, and **Fig. 3 (c)** shows the relative error between it and the response of the isotropic model. It can be found that the relative error is less than 1%, and the error is mainly from the responses at boundary. This further proves that anisotropy mainly leads to the overall rise of the response, and the existence of anisotropy mainly affects the nonlinear degree of the response near the boundary. Meanwhile, this also shows that the effect of thickness and anisotropy is not coupled, and the two can be treated separately in correction of AIL data.

Sensitivity of AIL Responses to Invasion

Apart from the influence of anisotropy, the impact of mud invasion in tight sandstone reservoirs is another crucial factor restricting the extraction of reservoir resistivity. To clarify the sensitivity of the AIL response to invasion, this section constructs a cylindrical layered model that only considers radial heterogeneity. The dipping angle of this model is 89°. Since the borehole effect has been eliminated during the pre-processing of AIL, only the invasion zone and the formation are considered in the radial direction of this model, with their resistivities being R_{xo} = 10 Ω·m and R_t = 20 Ω·m respectively. Assuming a maximum depth of invasion (DI) is 2m, the solid line in **Fig. 4 (a)** shows the characteristics of the AIL response as the DI changes. It can be found that invasion leads to the separation of the response of each detection depth, and the affect of response by invasion is inversely proportional to detection depth.

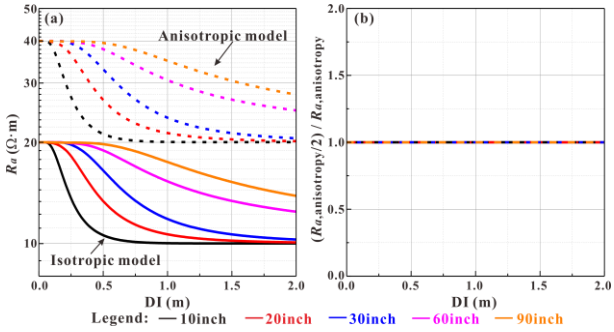

Fig. 4—(a) Comparison of responses in an isotropic invasion model with responses in an anisotropic invasion model; (b) Ratio of the responses of an isotropic invasion model to that of an anisotropic invasion model divided by the λ.

Based on the original model, the intrusion zone and formation resistivity are changed to the formation with λ= 2, that are, $R_{xo,v}$ = 40 Ω·m and R_v = 80 Ω·m. The dotted line in **Fig. 4 (a)** shows the responses of the anisotropic model. From the view of curve morphology, anisotropy still only leads to response rise, which is consistent with the previous conclusion. Divide the dashed line by the anisotropy coefficient and then divide it by the original model responses, as shown in **Fig. 4 (b)**, giving a ratio of 1 at each depth of invasion. This shows that the two effects of invasion and anisotropy are also decoupled.

Fig. 3 shows that the thickness causes a separation between AIL responses, which is similar to the effect of invasion on the responses. This makes it impossible to determine whether the two effects are coupled by response characteristic analysis alone. Therefore, we use the existing invasion inversion method to clarify the relationship between these two factors.

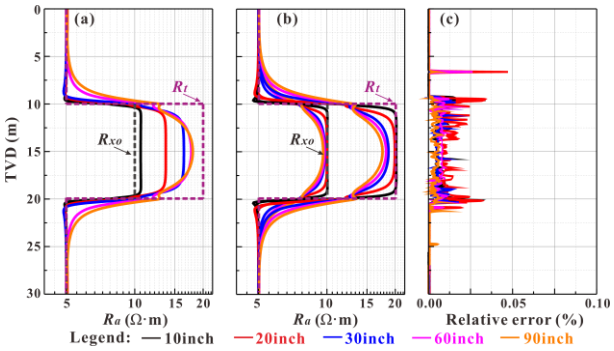

Fig. 5—(a) Responses of 3D model; (b) The model obtained by inversion and its reconstructed response; (c) Comparison of reconstructed responses with responses in 1D layered model.

We constructed a 3D model with a dipping angle of 89° and three layers in the vertical direction, all of which are isotropic media. In the radial direction, only the middle layer has invasion, *DI*= 0.5m, R_{xo}= 10 Ω·m, and R_t= 20 Ω·m. **Fig. 5 (a)** shows the responses of the 3D model calculated using the finite element method. Then, for the response in **Fig. 5 (a)**, the invasion inversion algorithm is used to obtain the invasion profile and the reconstructed AIL responses, as shown in **Fig. 5 (b)**. The reconstructed responses corresponding to the Rt after inversion is compared with the responses corresponding to the 1D layered model without invasion. **Fig. 5 (c)** shows the relative error between the two, which is less than 0.05%. This proves that the two effects of thickness and invasion can be hierarchical corrected.

TEUE THICKNESS CORRECTION

Since both layer thickness and intrusion effects can lead to separation in the measured response, the layer thickness effects need to be corrected first. In general, the AIL response is mainly affected by target layer and surrounding rock layer in HZ wells, and the contribution of distant layer is negligible. In this case, the multi-layer model can be equivalent to the three-layer model and the equivalent process is shown in **Fig. 6**.

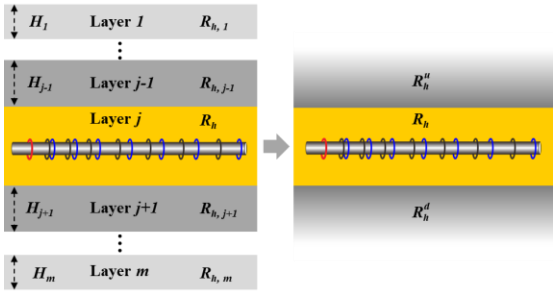

Fig. 6—Equivalent of a multi-layer model to a three-layer model in HZ wells.

The equivalent equation corresponding to the process of **Fig. 6** can be written as,

$$\frac{1}{R_h^u}=\frac{G_z\left(H_{j-1}\right)}{R_{h,j-1}}+\frac{G_z\left(H_{j-1}+H_{j-2}\right)-G_z\left(H_{j-1}\right)}{R_{h,j-2}}+\ldots+\frac{1-G_z\left(H_{j-1}+\ldots+H_1\right)}{R_{h,1}}, \quad (2)$$

where R_h^u is the resistivity of the upper surrounding rock layer equivalent to the target layer. $R_{h,i}$ and H_i are the resistivity and thickness of the i-th layer. G_z is the vertical integral geometric factor of 2ft resolution. The formula for obtaining the equivalent resistivity on the lower side layers is similar to **Eq. 2** and will not be repeated here. For the three-layer model, it is assumed that the resistivities of the upper and lower surrounding rocks is the same, and the resistivity contrast is set to $C = R_h / R_h^u$. Considering the effects of thickness H and resistivity contrast C, a series of three-layer models with α of 89° are constructed, and the corresponding focused responses of these models are calculated. On this basis, the true thickness correction coefficient TC of each focused response is calculated for each three-layer model. Take the 10inch response as an example, the formula for calculating its TC can be written as

$$TC_{i,j,k}^{10inch}=\frac{R_{h,i,j}}{R_{10inch}(C_i,H_j,TVD_k)}, \quad (3)$$

where R_{10inch} (C_i, H_j, TVD_k) is the 10inch response at the k-th TVD point of the middle layer, and the $R_{h,i,j}$ is the horizontal resistivity, where the resistivity contrast is C_i and the thickness is H_j. The true thickness correction coefficient is calculated for each focused response of each three-layer model, and the TC library can be obtained by using cubic spline interpolation method. **Fig. 7 (a)** and **Fig. 7 (b)** show the TC libraries of the 10inch and 90inch responses at the mid-point of the middle layer.

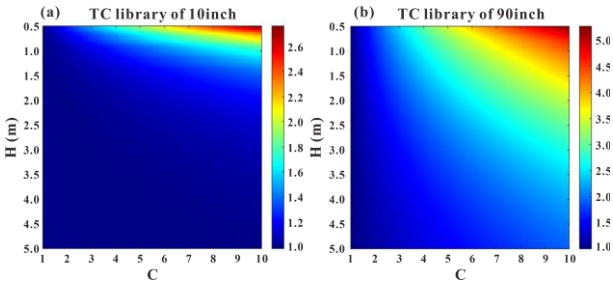

Fig. 7—TC libraries of focused responses: (a) 10inch; (b) 90inch.

As can be seen from **Fig. 7**, the degree to which the response is affected by the thickness increases with the detection depth, and is inversely proportional to the thickness and proportional to the resistivity contrast. In order to verify the effect of true thickness correction, take the model shown in **Fig. 3 (a)** as an example. True thickness correction was performed on the focused response, and **Fig. 8** shows the effect before and after true thickness correction. The corrected response is independent of thickness and accurately reflects true formation resistivity.

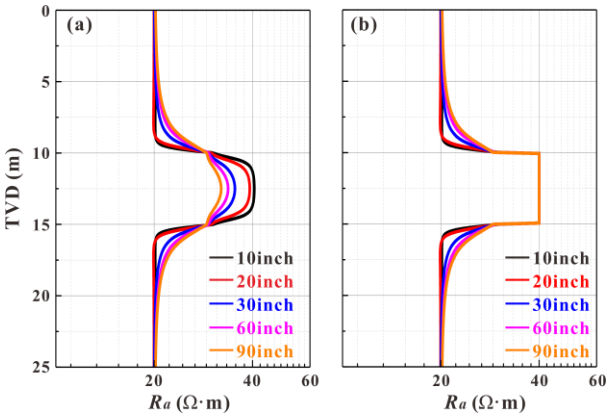

Fig. 8—Effect of true thickness correction with TC libraries: (a) Before correction; (b) After correction.

HIERARCHIAL CORRECTION METHOD

According to the above conclusions, the effects of thickness, anisotropy and invasion are not coupled. Therefore, the AIL data can first be corrected along the vertical or radial direction in HZ wells. Take the 3D model shown in **Fig. 9(a)** as an example, the middle layer of this model has the coupling effects of dipping angle, invasion, anisotropy and thickness. When the true thickness correction is applied to the middle layer, the 3D model can be decoupled into a combination of 1D horizontal layered model (shown in **Fig. 9(b)**) and 1D cylindrical layered model (shown in **Fig. 9(c)**). The effects of dipping angle, thickness and anisotropy are included in the former, and the latter is present to correct for the invasion effect. In **Fig. 9(c)**, R_t^e is the equivalent isotropic resistivity of R_t^h and R_t^v in **Fig. 9(a)**, i.e., $R_t^e = \sqrt{R_t^h * R_t^v}$. Similarly, $R_{xo}^e = \sqrt{R_{xo}^h * R_{xo}^v}$. On this basis, the horizontal layered model can be further reduced to a homogenous (0D) anisotropic model using the true thickness correction.

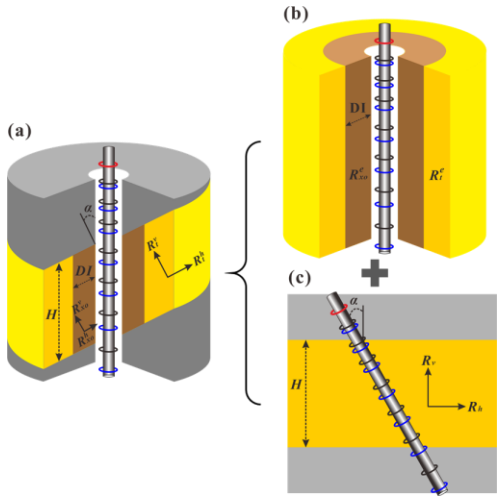

Fig. 9—(a) 3D inversion model; (b) 1D horizontal layered model; (c) 1D cylindrical layered model.

Next, a detailed description of the hierarchical correction of 3D AIL data is presented. Firstly, based on the measured AIL focused responses of HZ well, combined with the logging data of adjacent well sections and the geological background of the current reservoir, the thicknesses and horizontal resistivities of the target layer and the surrounding layers and dipping angle are obtained, and the 3D model of the HZ well can be established. Then, the relevant information is inputted into the true thickness correction coefficient library to correct the thickness effect of AIL response and obtain the responses affected by invasion and anisotropy. This process can eliminate the partial response separation. Furthermore, the thickness-corrected responses are inputted into the 1D cylindrical layered model, and a three-parameter inversion algorithm is used to obtain the depth of invasion *DI*, the equivalent isotropic invasion zone resistivity R_{xo}^e, and the equivalent isotropic formation resistivity R_t^e. Finally, the anisotropy coefficient is obtained by combining the equivalent isotropic formation resistivity R_t^e, the horizontal resistivity of adjacent well and the dipping angle, and is input into the 0D anisotropic inversion model to obtain the true horizontal resistivity R_h of the reservoir. The specific process of 3D AIL data correction is shown in **Fig. 10**.

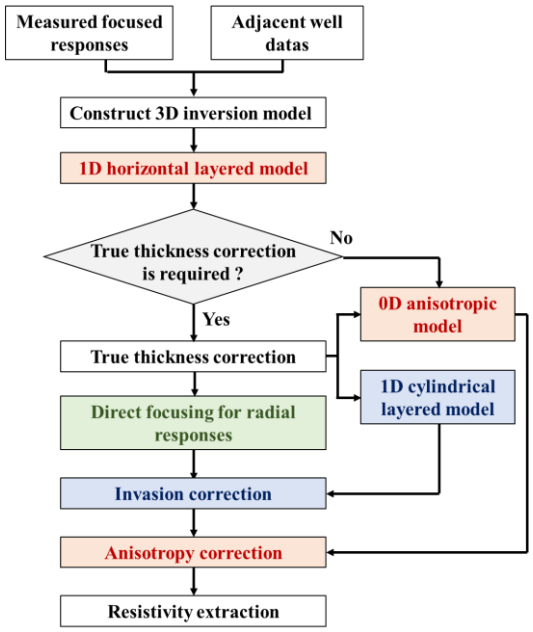

Fig. 10—Correction process of 3D AIL data in HZ wells.

In addition to the above analysis, this section will use 1D forward method to approximate 3D model response to further verify the feasibility of the hierarchical correction method. **Fig. 11 (a)** establishes a three-layer 3D model with a dipping angle of 80°. The surrounding rocks on the top and bottom of the model are isotropic media with resistivity of 5 Ω·m. The thickness of the middle layer is 3m, and there are mud invasion and anisotropy, where the DI= 0.2 m, $R_{xo,h}$= 5 Ω·m, $R_{xo,v}$= 10 Ω·m and the formation resistivities are R_h = 20 Ω·m, R_v = 40 Ω·m. The AIL response of this 3D model simulated using the

finite element method is given in **Fig. 11(b)**.

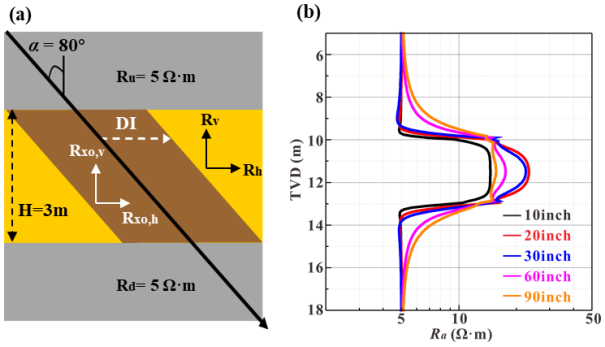

Fig. 11—(a) Three-layered 3D model; (b) Focused responses of the 3D model.

The equivalent horizontal resistivity corresponding to each detection mode in the middle-layer is calculated based on the radial integral geometric factor G_r with **Eq. (4)**.

$$R_h^e = \frac{R_{xo}^h \cdot R_t^h}{R_t^h \cdot G_r(DI) + R_{xo}^h \cdot \left[1 - G_r(DI)\right]}, \tag{4}$$

Furthermore, the same λ is used to obtain equivalent vertical resistivities of all detection mode. The equivalent resistivities corresponding to the 10inch detection mode are inputted into the 1D forward modeling algorithm of horizontal layered model, and the sub-array responses after skin effect correction can be obtained. Then, Express software is used to focus the sub-array responses, and the focused response of 10inch is selected as the result of the approximation calculation for the 10inch response of the 3D model. Repeat the above operation to obtain the approximation calculation results corresponding to other detection modes.

The comparison of the 1D approximation results (dotted line) and the 3D rigorous forward results (solid line) is shown in **Fig. 12 (a)**, and the relative error of the approximation calculation results is given in **Fig. 12 (b)**. It can be found that the relative error of each focused response is less than 3%, and the error is proportional to the magnitude of the response affected by the invasion. However, the calculation speed of 1D approximation is almost three orders of magnitude faster than the 3D forward modeling. This lays the foundation for the fast processing of 3D AIL data.

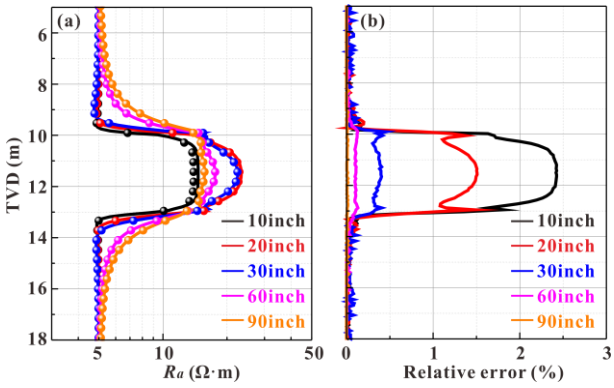

Fig. 12—(a) comparison of the 1D approximation results and the 3D forward results; (b) Relative error of the two method.

DIRECT FOCUSING FOR RADIAL RESPONSES

Both the 0D anisotropic inversion model after thickness correction and the 1D cylindrical layered inversion model do not need to consider the vertical effects. At this time, it is necessary to establish a new response focusing method which only considers radial factors. For the traditional SF algorithm, the principle of vertical focusing is to obtain the sub-array responses within a certain range of apparent depth above and below the current point, and then use the resolution differences among each sub-array response to compensate each other, so as to achieve the purpose of improving the resolution. Therefore, the effect of vertical focusing mainly depends on the vertical differences among the apparent depth points.

Due to the small vertical difference between the measured responses at different apparent depth points in HZ wells, the focusing effect of traditional SF algorithm is poor in HZ wells and cannot significantly improve the vertical resolution. Therefore, the vertical focusing in HZ wells is not necessary, and **Eq. (1)** can be simplified to 1D SF algorithm only considering radial factors, as shown in **Eq. (5)**.

$$\sigma_p(\rho_k) = \sum_{j=1}^{N} w_{k,j}\sigma_a(j). \tag{5}$$

The focusing coefficient $w_{k,j}$ in the **Eq. (5)** can be obtained by the radial integral geometric factors of the sub-array responses and the radial focused responses using polynomial fitting. To verify the accuracy of the

1D SF algorithm, **Fig. 13** presents a comparison of the focused responses calculated by the traditional SF algorithm and the 1D SF algorithm in a HZ well. In the figure, the first track (from left to right) is the dipping angle, about 89°, the second track is the apparent depth, the third track is the sub-array response after borehole correction, and the fourth track is the measured focused response with a vertical resolution of 2ft. By comparing the third and fourth tracks, it can be seen that the resolution of the focused response and the sub-array response are almost the same, which again proves that the vertical focusing is meaningless in HZ wells.

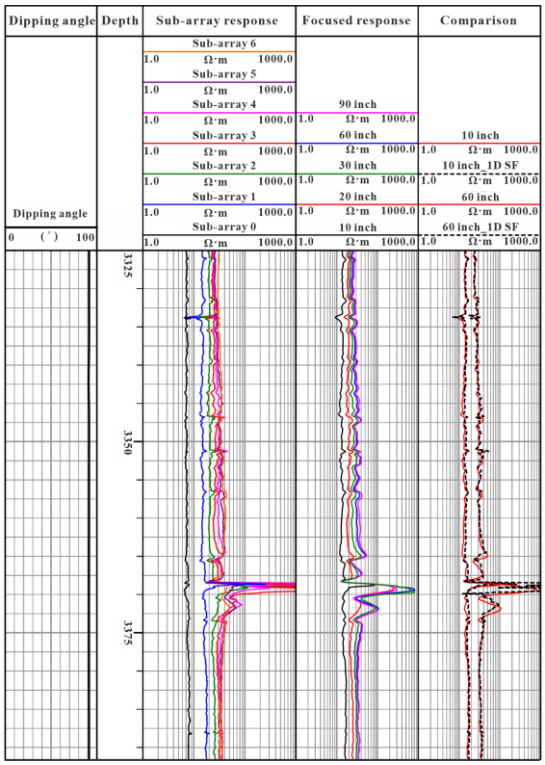

Fig. 13—Comparison of measured focused response and focused response calculated by 1D SF algorithm in HZ well.

In the fifth track, the measured focused response at the detection depth of 10inch and 60inch is compared with the response calculated by 1D SF algorithm for the sub-array response. The rules and values of the two are basically consistent. However, the sub-array response showed an abnormal "horn" near the depth of 3370m, which resulted in abnormal both the measured response and the 1D focusing response, possibly due to the presence of a high resistance layer on the upper side of the target layer and the proximity of the tool to the upper boundary.

ANSIORTOPY AND INVASION CORRECTION

Based on the hierarchical framework established in previous sections, the anisotropy and invasion effects in HZ wells can be decoupled and corrected sequentially. This section elaborates on the detailed workflow for anisotropy correction using the 0D anisotropic model and subsequent invasion correction via the cylindrical layered model.

The anisotropy correction begins with the 0D homogeneous model derived after true thickness correction. Generally, the anisotropy coefficient λ can be obtained in two ways, that is, through the drill core sampling of the target layer and combined determination based on the measured resistivity of multiple dipping angles. Considering the cost of measurement, the latter is usually chosen. Therefore, the λ is determined by comparing the measured responses of the HZ well with those from its vertical section, that is, the resistivity data of the adjacent well corresponding to the target layer, and its prediction formula can be written as,

$$\lambda = \frac{\sin\alpha}{\sqrt{\frac{R_{adj}^2}{R_a^2} - \cos^2\alpha}}, \tag{5}$$

where, α is the average value of the dipping angle in the HZ well, and sin and cos are the sine and cosine functions. R_{adj} is the measured resistivity of adjacent well, and the deep lateral response is generally adopted. R_a refers to measured AIL data in HZ well. Since the response of 10inch are seriously affected by the borehole and invasion, the responses of 20inch and 30inch is generally selected.

The Levenberg-Marquardt (L-M) algorithm is used to invert the 0D anisotropic model after the equivalence of each focused response, respectively. The horizontal resistivities corresponding to each response can be obtained separately. Then, these horizontal resistivities are inputted into the cylindrical layered model, and three-parameter inversion can be used to obtain the *DI*, R_{xo} and R_h.

To verify the efficiency of the new method, the response shown in **Fig. 11 (b)** is taken as an example and inverted using the hierarchical correction method proposed in this paper. In this example, the resistivity of the surrounding rock, the thickness and horizontal resistivity of target layer and dipping angle are known. First, we input the resistivity contrast between the surrounding rock and the

target layer and the thickness of the target layer into the coefficient library of true thickness correction to obtain the thickness correction coefficients for each focused response of the target layer. The responses after true thickness correction is shown in **Fig. 14**.

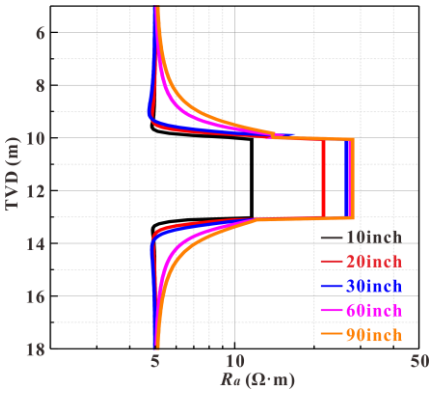

Fig. 14—The response shown in Fig. 8(b) after true thickness correction.

Then, the responses of each detection mode in the middle layer are extracted and inputted into the cylindrical layered inversion model, and the three-parameter inversion is used to obtain the *DI*, R_{xo}^{e}, and R_{t}^{e}, as shown in **Fig. 15 (a)**. Furthermore, the predicted anisotropy coefficient was obtained by inputting the equivalent formation resistivity R_{t}^{e}, the horizontal resistivity of the middle layer, and the dipping angle into the **Eq. (5)**. Predicted anisotropy factor of 1, with a relative error of 1% from the actual anisotropy coefficient. The anisotropy coefficient and horizontal resistivity were input to the 0D anisotropic inversion model, and the inverted horizontal resistivity R_h and vertical resistivity R_v are given in **Fig. 15 (b)**, and compared with the difference between R_h and the true horizontal resistivity R_h^{true}, with a relative error of about 2%.

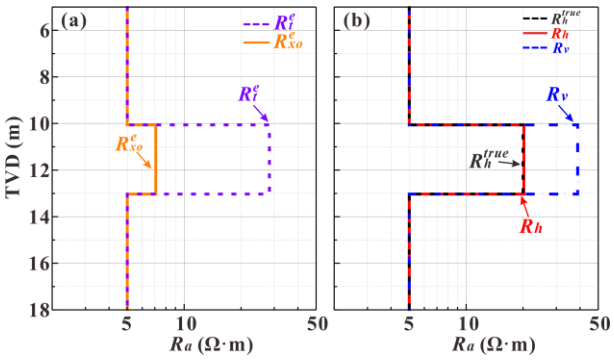

Fig. 15—(a) Invasion corrected results and the reconstructed focused responses of Rt; (b) Comparison of anisotropy correction results with true formation resistivity.

FIELD CASE

In order to verify the effectiveness of the classification correction method proposed in this paper, well-I in the tight sandstone reservoir shown in **Fig. 16** was selected as a test well. This well was measured using Baker Atlas HDIL tool with dipping angle about 86° (shown in the first track of **Fig. 16**). Core sampling results indicate that the anisotropy coefficient of the reservoir is 1.4. Adjacent well data show that the resistivity of this HZ well ranges from 20- 30 Ω·m, and the thickness is 6 m. The third track shows the measured AIL focused responses of 2ft resolution in this HZ section, and it can be noticed that the measured response is overall high when compared to the resistivity values indicated by the adjacent well. Meanwhile, due to the influence of mud invasion, the measured response shows obvious separation and disorder in the vicinity of 2100 m and in the section 2108- 2120 m.

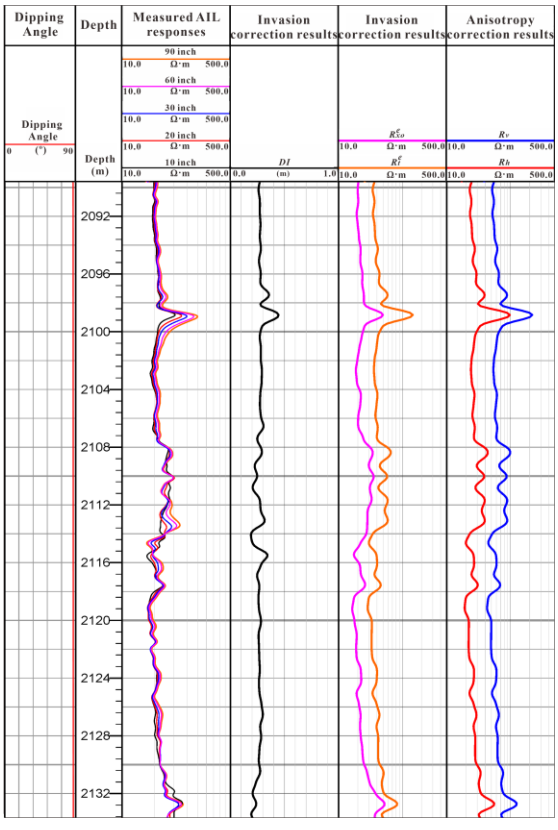

Fig. 16—Anisotropy and invasion correction results of AIL data

in tight sandstone well-I

Since there is almost no separation for the measured responses in the 2092-2096m section, it can be shown that the measured response in the absence of invasion is almost independent of the thickness. Therefore, the true thickness correction can be ignored during the processing of this example data to further improve the data processing speed. The *DI* at different depths obtained by the invasion correction are given in fourth track, and the R_{xo}^{e} and the R_{t}^{e} with the effect of anisotropy are inverted in fifth track. The anisotropy correction results are given in the sixth pass, and it can be seen that the anisotropy correction eliminates the overall rise of responses, and the corrected R_h is consistent with the resistivity of the adjacent well. During the processing of AIL responses from this HZ well, the inversion speed was approximately 4 logs/s.

Since we do not have other publicly available algorithms that can be used to process 3D HZ well data at this time, it is not possible to compare the accuracy of the new method at this time. However, through extensive theoretical simulations, the overall accuracy of the new method can be controlled within 3%. The parameters of computing platform used in this section are Windows 10 64-bit Professional 21H2 OS, an Intel(R) Core (TM) i9-9900 CPU, and 16GB memory. The computing software is Visual Fortran 2013.

SUMMARY AND CONCLUSIONS

In this research, a novel hierarchical correction method was developed to process AIL data in horizontal HZ wells within tight sandstone reservoirs. The complex 3D environment in HZ wells, with the combined effects of the dipping angle, mud invasion, resistivity anisotropy, and layer thickness, poses challenges to the interpretation of resistivity data. Through a detailed analysis of AIL responses, it was found that anisotropy mainly increases measured responses, mud invasion causes response disorder and separation, and layer thickness generally only leads to response separation. Notably, these three effects are not mutually coupled, validating the feasibility of the hierarchical correction approach for 3D data.

The newly developed method has multiple key contributions. It utilizes a coefficient library based on a 1D horizontal layered model for true thickness correction. A direct focusing algorithm for radial responses is introduced to speed up forward modeling. Moreover, the method performs sequential invasion and anisotropy corrections. The experimental results show that this method is highly effective, with an accuracy error controlled within 3%.

The practical application of this method in a tight sandstone reservoir field case was successful. It accurately characterized the invasion profile and extracted the true formation resistivity, showing good agreement with adjacent well data. Validation with measured data further confirmed its effectiveness, achieving a processing speed of four points per second. This provides a reliable foundation for fluid identification and reservoir evaluation in such reservoirs.

ACKNOWLEDGEMENT

This work was supported in part by the National Natural Science Foundation of China, Grant number 42474152, U23B2086 and 42374150; the Natural Science Foundation of Shandong Province, Grant number ZR2023MD053; the PetroChina Innovation Foundation, Grant number 2024DQ02-0152.

REFERENCES

Anderson, B. I., Barber, T. D., Luling, M. G., 1995. The Response of Induction Tools to Dipping, Anisotropic Formations. *Transactions of the SPWLA 36th Annual Logging Symposium*, Paper D.

Alpak, F. O., Dussan, V., Habashy, T. M., et al., 2003. Numerical simulation of mud filtrate invasion in horizontal wells and sensitivity analysis of array induction tools. *Petrophysics*, 44(6): 396 - 411. DOI: 10.3797/sciphysics.44.6 - 3

Barber, T. D., Rosthal, R. A., 1991. Using a multiarray induction tool to achieve high - resolution logs with minimum environmental effects. *SPE Annual Technical Conference and Exhibition*, SPE - 22725 - MS.

Beste, R., Hagiwara, T., King, G., et al., 2000. A New High Resolution Array Induction Tool. *SPWLA 41th Annual Logging Symposium*, SPWLA - 2000 - C.

Bang, J., Solstad, A., Mjaaland, S., 2001. Formation Electrical Anisotropy Derived from Induction - Log Measurements in a Horizontal Well. *SPE Reservoir Evaluation & Engineering*, 4(6): 483 - 488. DOI: 10.2118/ 75115-PA

Bai, Y., Yang, S. W., Ma, Y. G., et al., 2018. Adaptive Borehole Correction of Three-Dimensional Array

Induction Logging Data in a Vertical Borehole. *Chinese Journal of Geophysics*, 61(9): 3876 - 3888. DOI: 10.6038/cjg2018L0082

Gao, J., Zhao, A. B., Peng, F., et al., 2007. Inversion of Array Induction Logs and Its Application. *Petroleum Science*, 4(3): 31 - 35. DOI: 10.1007/s12182 - 007 - 0005 - x

Gorbatenko, A. A., Sukhorukova, K. V., 2016. High - Frequency Induction Logging in Deviated and Horizontal Wells: Geosteering and Inversion. *Russian Geology and Geophysics*, 57(7): 1111 - 1117. DOI: 10.1016/j.rgg.2016.06.010

Hou, J. S., Bittar, M., 2010. Correction for the Borehole Effect of Multi - component Array Induction Log Data. *PIERS 2010 Cambridge: Process in Electromagnetics Research Symposium Proceedings*.

Hagiwara, T., 2011. Apparent Dip and Apparent Anisotropy from Multifrequency Triaxial Induction Measurements. *Geophysics*, 76(1): F1 - F13. DOI: 10.1190/1.3511349

He, Z. B., Wu, D., Fan, Y., 2012. Skin Effect Correction Method of Multi - frequency Array Induction. *Natural Resources and Sustainable Development*, 361-363.

Hong, D. C., Li, N., Han, W., et al., 2021. An Analytic Algorithm for Dipole Electromagnetic Field in Fully Anisotropic Planar-Stratified Media. *IEEE Transactions on Geoscience Remote Sensing*, 59(11): 9120-9131. DOI: 10.1109/TGRS.2020.3040193

Løseth, L., Ursin, B., 2007. Electromagnetic Fields in Planarly Layered Anisotropic Media. *Geophysical Journal International*, 170: 44-80. DOI: 10.1111/j.1365-246X.2007.03390.x.

Li, H., Yuan, C., Li, C. L., et al., 2019. Pseudo - Focusing Processing of Array Induction Logging Measurements in High - Angle Wells. *the SPWLA 60th Annual Logging Symposium*, SPWLA - 2019 - IIIII.

Liu, Z. Y., Zhang, B. Q., Zhang, C. G., et al., 2020. Response Characteristics of an Array Induction Tool (HDIL) in Heterogeneous Anisotropic Formations. *Petrophysics*, 61(1): 72-85. DOI: 10.30632/PJV61N1-2020a2.

Mallan, R. K., Torres - Verdín, C., 2007. Effects of Geometrical, Environmental, and Petrophysical Parameters on Multi-Component Induction Measurements Acquired in High-Angle Wells. *Petrophysics*, 48(4): 271-288. DOI: 10.3797/ sciphysics. 48.4 – 1

Qiu, X., Tan, C., Lu, Y., et al., 2022. Evaluation of fractures using conventional and FMI logs, and 3D seismic interpretation in continental tight sandstone reservoir. *Open Geosciences*, 14(1): 530-543. DOI: 10.1515/geo-2022-0372

Rabinovich, M., Tabarovsky, L., Corley, B., et al., 2006. Processing Multi-Component Induction Data for Formation Dips and Anisotropy. *Petrophysics*, 47(6): 506 - 526. DOI: 10.3797/sciphysics.47.6 - 5

Tarouilly, L., Rabinovich, M., Wang, T., et al., 2003. 3D Simulation of Array Induction Logging in a Deviated Well Environment: A Mahakam Delta Case Study. *SPE Annual Technical Conference and Exhibition*, SPE - 84600 - MS.

Wang, H. N., 2009. Adaptive Regularization Iterative Inversion of Array Multicomponent Induction Well Logging Datum in a Horizontally Stratified Inhomogeneous TI Formation. *IEEE Transactions on Geoscience and Remote Sensing*, 49(11): 4483 - 4492. DOI: 10.1109/TGRS.2011.2142187

Wang, L., Deng, S. G., Xie, G. B., et al., 2022. A New Deep - reading Look - ahead Method in Electromagnetic Logging - While - Drilling Using the Scattered Electric Field from Magnetic Dipole Antennas. *Petroleum Science*, 19(1): 180 - 188. DOI: 10.1016/ j.petsci. 2021.09.035

Wang, L., Qiao, P., Li, Z. Q., et al., 2023. A New Semianalytical Algorithm for Rapid Simulation of Triaxial Electromagnetic Logging Responses in Multilayered Biaxial Anisotropic Formations. *Geophysics*, 88(2): D115 - D129. DOI: 10.1190/ GEO2021-0714.1

Zhou, Q., Beard, D., Hilliker, D. J., 1994. Induction Tool Resolution. *SEG Technical Program Expanded Abstracts*.

Zhou, J., Li, H., Rabinovich, M., et al., 2016. Interpretation of Azimuthal Propagation Resistivity

Measurements: Modeling, Inversion, Application and Discussion. *the SPWLA 57th Annual Logging Symposium*, SPWLA-2016-HHHH.

Zhou, F., Meng, Q. X., Hu, X. Y., et al., 2016. Evaluation of Reservoir Permeability Using Array Induction Logging. *Chinese Journal of Geophysics*, 59(11): 4360 - 4371. DOI: 10.6038/cjg20161136

ABOUT THE AUTHOR

Ping Qiao is a Ph.D. student in Geological Resources and Geological Engineering of China University of Petroleum (East China). His research involves the fast forward modeling of induction logging and inversion of induction logging data in horizontal well.

Lei Wang , Ph.D., is an associate professor at the School of Geosciences and Technology, China University of Petroleum (East China). His research interests include the electromagnetic detection in wells, fast forward and inversion technology and geosteering while drilling.

Yingming Liu, Ph.D., graduated from the Petroleum Exploration and Development Research Institute in 2011, majoring in Geological Exploration and Information Technology. His main research interests are logging data processing and software development.

Xiaokai Xu, Ph.D., graduated from China University of Petroleum (East China) in 2012, majoring in Geological Resources and Geological Engineering. He has long been engaged in the research and development of acoustic logging detection equipment.

Xiyong Yuan, Ph.D., is an associate Researcher at Sinopec Matrix Corporation. His research interests include electrical logging theory, method and interpretation.

Fuhua Cao is a M.Eng. student in Geological Engineering of China University of Petroleum (East China). His main research interests are induction logging and 3-D finite difference modeling.